

## **Control of Flow and Heat Transfer by Jets with Self-Excited Oscillation or Longitudinal Vortex Generation**

Kazuyoshi NAKABE (中部主敬)

Department of Mechanical Engineering, Kyoto University  
Kyoto 606-8501, Japan  
Tel & Fax: 075-753-5251  
E-mail: nakabe@htrans.mech.kyoto-u.ac.jp

Two kinds of jet nozzle configuration were proposed to design jet devices for the control of impingement heat transfer, and the heat transfer performances of those impinging jets were investigated with the image conversion technique of thermochromic liquid crystal colors into target wall temperatures. One nozzle is equipped with a coaxial extension collar at the nozzle exit to construct a sudden step expansion and produce acoustically self-excited oscillations. The other is applied to an impinging jet into a crossflow, which was flush-mounted on a duct wall surface with pitch and skew angles to obliquely discharge the jet fluid and intentionally generate longitudinal vortices. It was found in the case of the former nozzle that main and secondary peaks of the Nusselt number distributions around the stagnation region were merged into a single peak as the extension collar length was increased, regardless of the oscillating frequency. The latter case was found to enhance heat transfer from a spanwisely much wider area, compared with the case of the conventional impinging jet nozzle normal to the target wall. The enhanced area of heat transfer corresponds very well to the behaviors of the longitudinal vortices. The experimental results obtained in the present study could be offered as good database to examine numerical computation of jet impingement heat transfer.

### **1. Introduction**

Jet impingement is one of the well-established cooling or drying techniques in a wide variety of industrial applications, and has greater advantages to enhance and control local heat and mass transfer from a target wall than convective flows parallel to the wall surface. Thus, many experimental research works have been conducted to investigate flow and heat transfer characteristics of the impinging jets. Gardon and Akfirat [1] made extensive measurements of the average and local heat transfer coefficients produced by two-dimensional jet impingement for both cases of a single slot jet and arrays of slot jets. They also examined the role of turbulence in the heat transfer mechanism of jet impingement [2]. Martin [3,4] has reported a comprehensive survey of early research works as well as some optimum design proposals of heat exchanger and dryer with experimental data for single round or slot jets and also for arrays of round or slot jets. Later, Goldstein et al. [5] have investigated both heat transfer and recovery factor distributions of a round impinging jet and also summarized the previous experimental works on jet impingement heat transfer.

Jet impingement, however, has some disadvantages that the heat transfer rapidly deteriorates outside the impinging region. Excess fluid flow rate through a jet nozzle or multiple jets should be needed to enhance or control the heat transfer from wide areas away from the jet stagnation region which is sometimes inevitably exposed to an excessively cool environment. In the present study, a jet nozzle equipped with a coaxial

extension collar to construct a sudden step expansion will be proposed and examined to see if such a nozzle has a capability to enhance and control the local heat transfer rates of an impinging jet or not. Seyed-Yagoobi [6,7] only reported that a similar jet nozzle generates acoustically self-excited oscillations and the jet through the nozzle is beneficial for heat transfer at optimum nozzle-to-impingement surface spacing.

Heat transfer rates of impinging jets are also deteriorated by a crossflow which is inevitably produced as the result of the confluence of the jets discharged upstream. Then, the impinging jets situated downstream of the upstream jets are deflected before impingement, directed at an oblique incidence angle relative to the target surface, and thermally influenced by the interaction of the crossflow. Effects of the crossflow on the heat transfer of impinging jet normal to the target surface were investigated by Metzger and Korstad [8], Sparrow et al. [9], Bouchez and Goldstein [10], Goldstein and Behbahani [11] etc. Such situations of jet impingement are seen, for example, inside a gas turbine vane where the cooling paths are situated between the inner surface of the vane and the outer surface of 'insert' mounted in the vane to feed coolant air from outside. Jets discharged from many small holes drilled in the insert impinge onto the inner surface of the vane. The outside surface temperature,  $T_{wo}$ , of the vane exposed to hot burnt gas from a combustor could be estimated with one-dimensional steady-state heat balance assumption to be as shown below:

$$T_{wo} = \frac{l/\lambda + 1/\alpha_i}{1/\alpha_f + (l/\lambda + 1/\alpha_i)} (1 - \eta_f) T_g + \frac{1/\alpha_f + \eta_f (l/\lambda + 1/\alpha_i)}{1/\alpha_f + (l/\lambda + 1/\alpha_i)} T_c, \quad \eta_f = \frac{T_g - T_f}{T_g - T_c}$$

$T$ ,  $l$ ,  $\lambda$ ,  $\alpha$ ,  $\eta$ , respectively, denote temperature, vane thickness, thermal conductivity of vane material, heat transfer coefficient and film cooling efficiency. Subscripts  $g$ ,  $c$ ,  $f$  and  $i$  indicate, respectively, burnt gas outside of the vane, coolant gas from the insert, film cooling and inside surface of the vane. Thus, the increment of the burnt gas temperature,  $\Delta T_g$ , could be related to the increment of heat transfer coefficient,  $\Delta \alpha_i$ , on the inner surface of the vane with the following equation.

$$\Delta T_g = \frac{T_{wo} - T_f}{(1 - \eta_f) \alpha_f (l/\lambda) (\alpha_i l/\lambda + 1)} \times \left\{ 1 - \frac{\alpha_i + \lambda/l}{\Delta \alpha_i + \alpha_i + \lambda/l} \right\} T_c \quad (1)$$

Turbine inlet temperature is one of the most important parameters to raise the thermal efficiency of gas turbine, considered to be as the burnt gas temperature in this case. According to the above equation, the temperature gain,  $\Delta T_g$ , is increased with a decrease in the reciprocal of the heat transfer coefficient  $\Delta \alpha_i$ , while no gain of  $\Delta T_g$  occurs at  $\Delta \alpha_i = 0$ . Thus, it is clearly understand that the heat transfer from the inner surface should be enhanced to raise the thermal efficiency of gas turbine. Addition of impinging jet to a main flow increases a time- and space-averaged heat transfer coefficient, for example, from 11.5 to 40.9W/(m<sup>2</sup>K) obtained experimentally under the jet Reynolds number = 40,000, which corresponds to the rise of the turbine inlet temperature up to 1,400°C according to Eq. (1).

Geometrical constraint on the locations of jet nozzle and target surface also results in oblique jet impingement. Effects of oblique incidence angles on impingement heat

transfer characteristics were investigated by Sparrow and Lovell [12], Goldstein and Franchett [13], Ozdemir and Whitelaw [14] etc. Obliquely discharged jet into crossflow generated by the above-mentioned confluent flows were also investigated by some other researchers including Huang et al. [15]. In such cases, the pitch angle, defined as the inclination angle of the jet injection vector relative to its projection vector onto the jet-installed surface, has usually a certain fixed value, while the skew angle, defined as the orientation angle of the jet projection vector relative to the crossflow direction vector, is always set to be zero, that is, parallel to the crossflow. The authors previously introduced the skew angle to the jet orientation for jet impingement heat transfer, and made the flow visualization that the impinging jet with such compound angle orientation discharged into crossflow generates a pair of counter-rotating longitudinal vortices [16, 17]. A similar attempt with such a compound angle orientation was made experimentally by Johnston and Nishi [18], Compton and Johnston [19], Ligrani et al. [20] and Lee et al. [21] and numerically by Zhang [22] and Zhang and Collins [23]. Their objective, however, was momentum and heat transfer control only near the nozzle-installed surface, examples of which include the suppression of flow separation from air foil surface and the film cooling of gas turbine blades and vanes. As the second topic in the present study, the heat transfer mechanism of the innovative jet impinging obliquely onto the jet-facing target surface will also be investigated together with the flow visualization of the interaction between two obliquely impinging jets situated separately in the crossflow direction.

## 2. Impinging Jet through the Nozzle with a Sudden Step Expansion

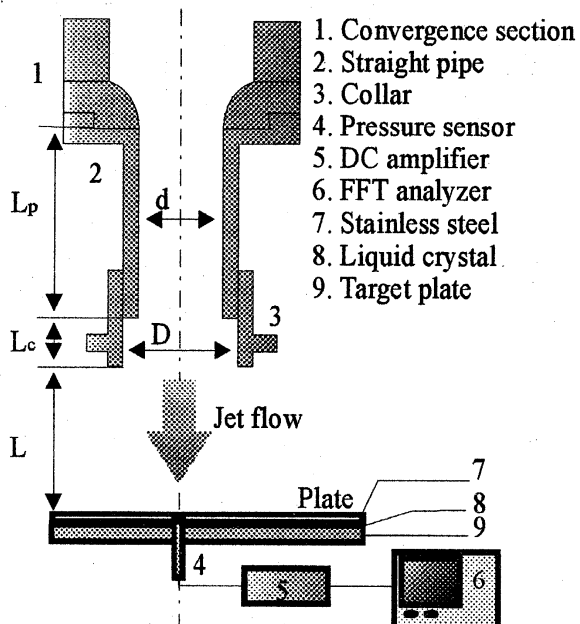


Fig. 1 Experimental apparatus.

Figure 1 shows a schematic illustration of the experimental apparatus used in the case of sudden step expansion nozzle. A coaxial extension collar flange 3 is installed to construct the sudden step expansion at the exit of a conventional straight pipe nozzle, the inner and outer diameters of which are  $d = 20\text{mm}$  and  $D = 30\text{mm}$ , respectively. The working fluid was air. The jet Reynolds numbers based on the outer diameter was set to be 40,000 and 50,000. An impinging distance  $L$  was changed in three steps,  $L/D = 4/3$ ,  $8/3$  and 4. The length of the extension collar  $L_C$  can be slid on the outer surface of the straight pipe nozzle to suitably adjust the length for sound-generation tuning without any change of the impinging distance. Pressure signals at the stagnation point were monitored with a probe of silicon diaphragm pressure transducer (XCQ-062, Kulite Semiconductor Products Inc.).

Semiconductor Products Inc.).

The power spectra derived from the pressure signals are shown in Fig. 2. The jet Reynolds number was set to be 40,000, and the impinging distance ratio  $L/D = 4/3$ . The prominent frequency component  $f$  of the spectra was found to be around 1.0kHz, almost independent of the collar length under the present geometrical conditions, while the intensity of the frequency component strongly depends on the collar length. The

maximum intensity was obtained in the case of  $L_c = 36\text{mm}$ , and the second maximum in the case of  $L_c = 65\text{mm}$ . The power spectrum of the same diameter straight pipe nozzle without the extension collar was also monitored, which shows a completely different spectrum distribution with a considerably low prominent frequency.

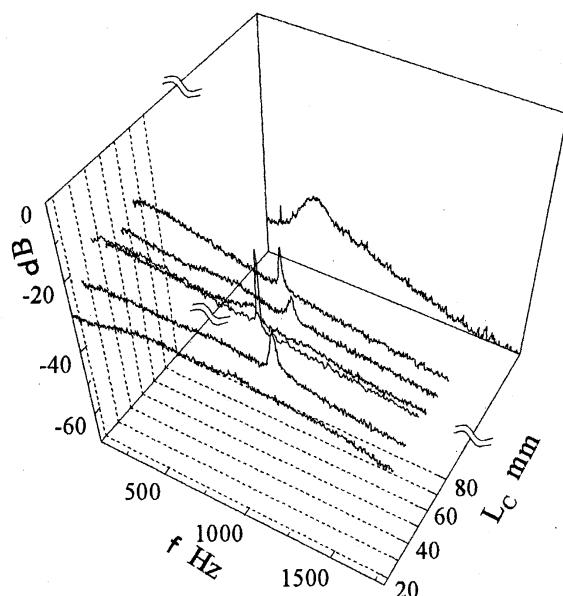


Fig. 2 Power spectra ( $Re_c = 40,000$  and  $L/D = 4/3$ ).

The heat transfer target plate 7 described in Fig. 1 was made of transparent acrylic resin, and stainless steel strips were glued on the surface of the plate to heat up electrically. Thermochromic liquid crystal sheets were sandwiched in between the target wall and the stainless steel strips to monitor the surface temperatures of the target plate. The color images of the liquid crystal sheets were captured with a color CCD camera through the transparent target plate outside of the test section, and converted into temperature distributions by making use of supervised learning algorithm of hierarchy neural network system [16]. The calibration of the image conversion method was done using reference temperatures measured by K-type thermocouples prior to every heat transfer experiment. The standard deviation between the output temperature of the neural network system and the reference temperature directly

measured by the thermocouples was  $0.18\text{K}$  at any temperature in the chromatic temperature range of the liquid crystal from  $26.5^\circ\text{C}$  to  $43.5^\circ\text{C}$ .

Figure 3 shows local Nusselt number distributions on the jet impingement target plate. The experimental conditions were same as the ones described in Fig. 2. Case (a) was obtained for a straight pipe nozzle without the extension collar. The inner diameter of this straight pipe nozzle was  $30\text{mm}$  as same as the inner diameter of the extension collar. Case (b), (c), (d) and (e) correspond to the results of the cases of the extension collar length  $L_c = 16\text{mm}$ ,  $26\text{mm}$ ,  $44\text{mm}$  and  $65\text{mm}$ , respectively. As clearly seen in these Nusselt number distributions, all cases with the sudden step expansion enhance the impingement heat transfer much more around the jet stagnation area, compared with the case with the straight pipe nozzle.

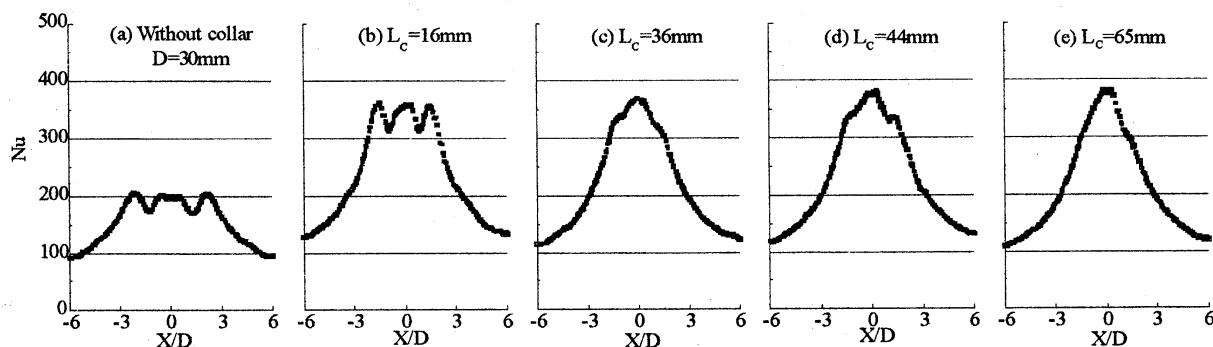


Fig. 3 Nusselt number distributions ( $Re_c = 40,000$  and  $L/D = 4/3$ ).

Another interesting feature observed in Fig. 3 is that the patterns of the local Nusselt number distributions are modified depending on the length of the extension collar. It was observed that there symmetrically exists a secondary peak on the shoulder of the Nusselt number distribution, in particular, for Case (a) and also for Case (b). The Nusselt numbers at the secondary peaks for both cases were almost equal to the one at a central main peak. The value of the main peak was almost same, regardless of the extension collar length. The secondary peak, however, was gradually buried in the Nusselt number distribution to be merged into a single peak with an increase in the extension collar length. As mentioned above in Fig. 2, the most and the second most intense acoustic sounds were obtained at the prominent frequency 1.0kHz in Case (c) and at 0.92kHz in Case (e), respectively. In spite of this acoustic sound generation, the Nusselt number distribution scarcely showed remarkable changes in these two cases. Thus, it was conjectured from the results obtained here that the self-excited oscillation might have only an auxiliary effect on the jet impingement heat transfer under the present experimental conditions. These results also give us the further inference that the precession of the jet flow along the inner surface of the extension collar due to the Coanda effect could level the unevenness of the Nusselt number distribution near the stagnation area. Much further measurements and investigations of heat transfer including flow visualization should be required.

### 3. Inclined Impinging Jet into Crossflow

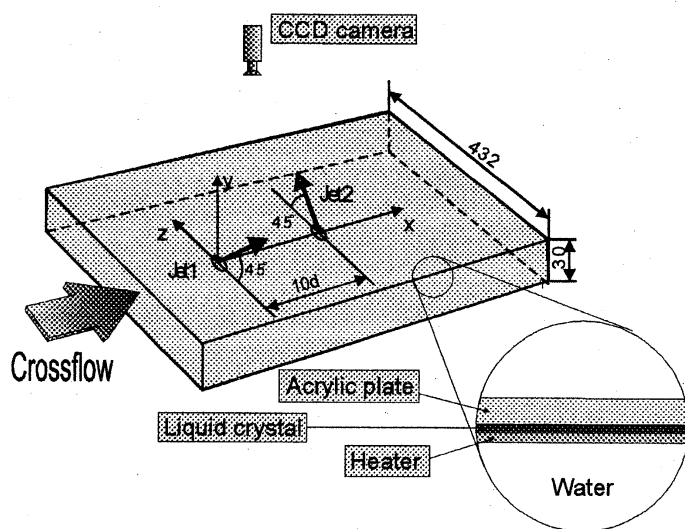


Fig. 4 Test section of inclined impinging jets.

The flow configuration of the inclined impinging jets was illustrated in Fig. 4. The jet nozzle with an oval cut end was mounted flush with the bottom wall surface of the test section made of transparent acrylic material. Dimensions of the test section are also shown in Fig. 4 together with some geometric parameters, the jet nozzle arrangement and the coordinate system used here. The jets discharged from the nozzle obliquely impinge onto the top wall of the test section with the above-defined pitch angle  $\phi$  raised from the bottom wall and the skew angle  $\theta$  relative to the crossflow. The two jets, Jet 1 and Jet 2, have the same dimensions except the skew angle.

The pitch was fixed at 45 degrees for both jets, while the skew angle at 90 degrees for Jet 1 and at  $-90$  degrees for Jet 2. Jet 2 was situated  $10d$  downstream of Jet 1, where  $d$  indicates the jet nozzle diameter, 6.0mm.

The origin of the coordinate system is located at the center of the open end of Jet 1.  $x$ ,  $y$  and  $z$  designate, respectively, the streamwise, normal and spanwise coordinates. The Reynolds number of the crossflow,  $Re_c$ , based on the hydraulic diameter of the test section was changed in three steps, 3,000, 4,000 and 5,000. The velocity ratio of the jet to the crossflow,  $VR$ , was changed also in three steps, 3, 5 and 7.

Cross-sectional patterns of the flows were visualized by shining a thin sheet of

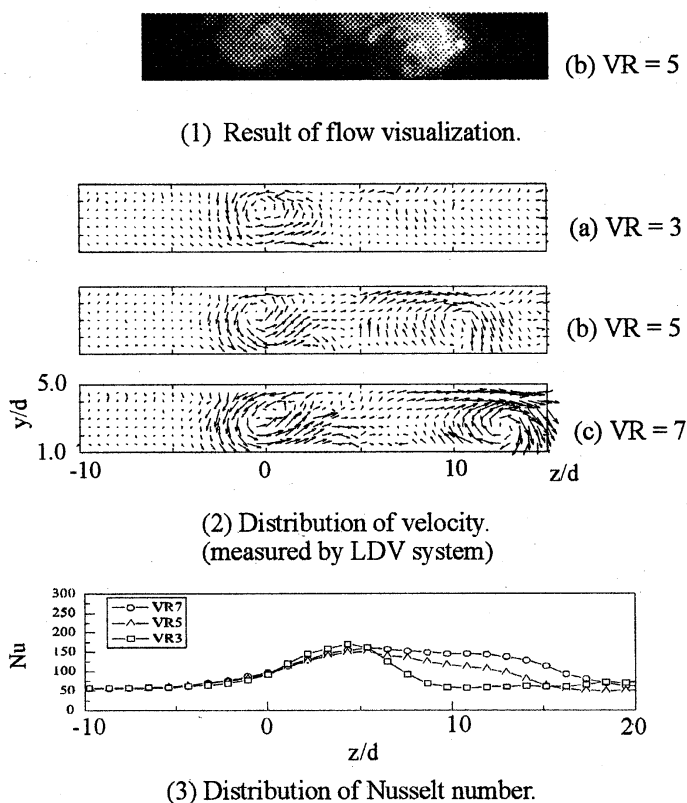


Fig. 5 Cross-sectional distributions ( $Re_c = 5,000$  and  $x/d = 20$ ).

5 was shown in the same figure. All views of the maps show the flow patterns viewed from the downstream end of the test section.

What is evident from the snapshot taken here is that there exists a pair of counter-rotating longitudinal vortices. The velocity vectors correspond very well to the locations of the longitudinal vortices described in the snapshot image. The right-hand side of the Nusselt number distribution becomes a plateau-like shape in the wide spanwise range with an increase in the VR value, which corresponds to the behaviors of the clockwise rotating vortex. The detail comparison between the Nusselt number distributions and the velocity vector maps reveals that the enhanced region of heat transfer corresponds to the regions including the noticeable wallward flow region near the target wall surface and the strong spanwise flow region sweeping the surface of the target wall. Streamwise flows with relatively high velocities were also observed in this region, although the velocity distributions are not described in this paper. The wallward flow was intensified by the anti-clockwisely rotating longitudinal vortex, the location of which seems to be almost independent of the VR ratio. This anti-clockwise vortex may have similar characteristics observed by Johnston et al. [18, 19] that the interaction of such an oblique jet with the crossflow comprising a turbulent boundary layer produces a longitudinal vortex which remains well downstream and enhances cross-stream mixing. They, therefore, proposed that the oblique jet could be applied to the control of turbulent boundary layer separation or stall control on the jet nozzle-installed wall.

Figure 6 shows example of the contours of local Nusselt numbers for the three

Argon-ion laser light through fluorescent dyes which were premixed into the crossflow. The flow patterns were time-sequentially captured from the downstream with a commercially available color CCD video camera, and the image processing of some featured frames was conducted to investigate the flow structures and also the interaction of the two jets. The temperatures of the target wall surface were measured with the color-to-temperature conversion technique mentioned in the previous section, according to Ref. [16]. The distributions of time-averaged velocity and its fluctuation components were also measured using two-color fiber laser Doppler anemometry.

Figure 5 shows the time-averaged flow velocity vector maps (b) corresponding to the spanwise Nusselt number distributions (3) obtained at  $x/d = 20$  for three different VR values, 3, 5 and 7, under the flow condition of  $Re_c = 5,000$  for a single inclined impinging jet. A snapshot (a) of the cross-sectional dye-added jet taken in the case of VR =

different cases of the two oblique jets, Jet 1 and Jet 2, arranged at the streamwise distance of 10 nozzle diameters. The contours of (a), (b) and (c) correspond to the velocity ratios  $VR = 3, 5$  and  $7$ , respectively, under the constant crossflow Reynolds number,  $Re_c = 3,000$ . The indexed gray scales correspond to the values of the Nusselt number  $Nu$ . It was observed that the heat transfer enhancement region ( $Nu > 100$ ) has two peaks of the Nusselt number distribution, each position of which will be around the stagnation point of each oblique jet. The enhanced regions of heat transfer may correspond well to the regions where longitudinal vortices exist.

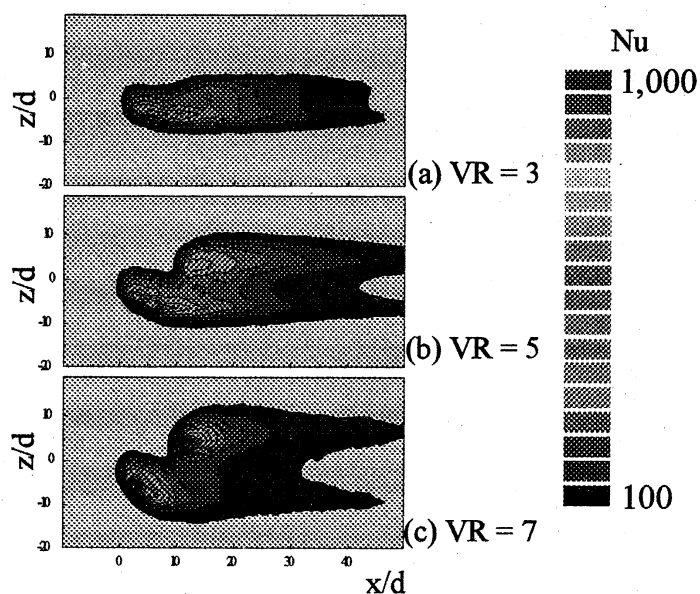


Fig. 6 Nusselt number contours ( $Re_c = 3,000$ ).

Close observation in each figure reveals that the downstream peak produced by Jet 2 located downstream of Jet 1 is relatively lower than the upstream one in the present flow conditions. The heat transfer performance of Jet 2 could be modified through the flow interaction with the longitudinal vortices generated by Jet 1.

#### 4. Conclusions

Two kinds of jet nozzle configuration were proposed to design jet impingement devices for heat transfer augmentation, and the heat transfer performances of those impinging jets were investigated with the image conversion technique of thermochromic liquid crystal colors into target wall temperatures. The nozzle with the sudden step expansion was found to generate acoustically self-excited oscillations with the prominent frequency around 1.0kHz. The main and secondary peaks of the Nusselt number distributions around the stagnation region were merged into a single peak as the extension collar length was increased, regardless of the prominent frequency.

The inclined impinging jet with compound discharging orientations was found to generate a pair of intense counter-rotating longitudinal vortices and also to have a beneficial heat transfer performance. It was found that the heat transfer of the inclined jet was enhanced on the wider area of the target wall, compared with the case of the conventional impinging jet nozzle normal to the target wall. The enhanced area of heat transfer corresponds very well to the behaviors of the longitudinal vortices.

#### References

- [1] R. Gardon and J.C. Akfirat, Heat transfer characteristics of impinging two-dimensional air jets, *Trans. ASME: J. Heat Transfer*, 88 (1966), pp. 101 - 108.
- [2] R. Gardon and J.C. Akfirat, The role of turbulence in determining the heat-transfer

- characteristics of impinging jets, *Int. J. Heat Mass Transfer*, 8 (1965), pp. 1261 - 1272.
- [3] H. Martin, Impinging jet flow heat and mass transfer, *Advances in Heat Transfer*, 13 (1997), pp. 1 - 60.
- [4] H. Martin, Impinging jets, *Heat Exchanger Design Handbook*, 2 (1983), pp. 2.5.6-1 - 2.5.6-10.
- [5] R.J. Goldstein, A.I. Behbahani and K.K. Heppelmann, Streamwise distribution of the recovery factor and the local heat transfer coefficient to an impinging circular air jet, *Int. J. Heat Mass Transfer*, 29-8 (1986), pp. 1227 - 1235.
- [6] J. Seyed-Yagoobi, Enhancement of heat and mass transfer with innovative impinging jets, *Drying Technology*, 14-5 (1996), pp. 1173 - 1196.
- [7] J. Seyed-Yagoobi and R.H. Page, Enhancement of heat transfer with innovative impinging jets, *Proc. 10<sup>th</sup> Int. Symp. on Trans. Phenomena in Thermal Science and Process Engineering*, 2 (1997), pp. 343 - 348.
- [8] D.E. Metzger and R.J. Korstad, Effects of crossflow on impingement heat transfer, *Trans ASME; J. Engineering for Power*, 94 (1972), pp. 35 - 42.
- [9] E.M. Sparrow, R.J. Goldstein and M.A. Rouf, Effect of nozzle - surface separation distance on impingement heat transfer for a jet in a crossflow, *Trans. ASME: J. Heat Transfer*, 97 (1975), pp. 528 - 533.
- [10] J.-P. Bouchez and Goldstein, Impingement cooling from a circular jet in a cross flow, *Int. J. Heat Mass Transfer*, 13 (1975), pp. 719 - 730.
- [11] R.J. Goldstein and A.I. Behbahani, Impingement of a circular jet with and without cross flow, *Int. J. Heat Mass Transfer*, 25-9 (1982), pp. 1377 - 1382.
- [12] E.M. Sparrow and B.J. Lovell, Heat transfer characteristics of an obliquely impinging circular jet, *Trans. ASME: J. Heat Transfer*, 102 (1980), pp. 202 - 209.
- [13] R.J. Goldstein and M.E. Franchett, Heat transfer from a flat surface to an oblique impinging jet, *Trans. ASME: J. Heat Transfer*, 110 (1988), pp. 84 - 90.
- [14] I.B. Ozdemir and J.H. Whitelaw, Impingement of an axisymmetric jet on unheated and heated flat plates, *J. Fluid Mech.*, 240 (1992), pp. 503 - 532.
- [15] Y. Huang, S.V. Ekkad and J.-C. Han, Detailed heat transfer coefficient distributions under an array of inclined impinging jets using a transient liquid crystal technique, *Proc. 9<sup>th</sup> Int. Symp. on Transport Phenomena in Thermal-Fluids Eng., II* (1996), pp. 807 - 812.
- [16] K. Nakabe, A. Higashio, W. Chen, K. Suzuki and J.H. Kim, An experimental study of the flow and heat transfer characteristics of longitudinal vortices induced by an inclined impinging jet into a crossflow (Measurements of heat transfer coefficients using thermochromic liquid crystal), *Proc. 11<sup>th</sup> Int. Heat Transfer Conference*, 5 (1998), pp. 439 - 444.
- [17] K. Nakabe, K. Suzuki, K. Inaoka, A. Higashio, J.S. Acton and W. Chen, Generation of longitudinal vortices in internal flows with an inclined impinging jet and enhancement of target plate heat transfer, *Int. J. Heat Fluid Flow*, 19 (1998), pp. 573 - 581.
- [18] J.P. Johnston and M. Nishi, Vortex generator jet - Means for flow separation control, *AIAA J.*, 28-6 (1990), 989 - 994.
- [19] D.A. Compton and J.P. Johnston, Streamwise vortex production by pitched and skewed jets in a turbulent boundary layer, *AIAA J.*, 30-3 (1992), pp. 640 - 647.
- [20] P.M. Ligrani, J.M. Wigle, S. Ciriello and S.W. Jackson, Film-cooling from holes with compound angle orientations: Part 1; Part 2, *Trans. ASME: J. Heat Transfer*, 116 (1994), pp. 341 - 352; pp. 353 - 362.
- [21] S.W. Lee, J.R. Byun and D.S. Lee, Measurements of temperature fields within film-

- cooling jets in a row with compound angle orientations, 3 (1996), pp. 83 - 88.
- [22] X. Zhang, Interaction between a turbulent boundary layer and elliptic and rectangular jets, *Eng. Turbulence Modeling and Experiments 2* (Eds. W. Rodi and F. Martelli), (1993), pp. 251 - 260.
- [23] X. Zhang and M.W. Collins, Flow and Heat Transfer in a Turbulent Boundary Layer through Skewed and Pitched Jets, *AIAA J.*, 31-9 (1993), pp. 1590 - 1599.